AUTHOR(S): ZHANG, Z., KIM, C., FERNANDEZ, C., SUNDARAM, M.M., RAMAKRISHNAPPA, T., WANG, Y., WANG, L., SUN, T. and HU, X.

TITLE: Adsorption removal of methylene blue from aqueous solution on carbon-coated Fe3O4 microspheres functionalized with chloroacetic acid.

YEAR: 2018

Publisher citation: ZHANG, Z., KIM, C., FERNANDEZ, C., SUNDARAM, M.M., RAMAKRISHNAPPA, T., WANG, Y., WANG, L., SUN, T. and HU, X. 2018. Adsorption removal of methylene blue from aqueous solution on carbon-coated Fe3O4 microspheres functionalized with chloroacetic acid. Science and engineering of composite materials [online], 25(2), pages 353-361. Available from: https://doi.org/10.1515/secm-2016-0138

OpenAIR citation: ZHANG, Z., KIM, C., FERNANDEZ, C., SUNDARAM, M.M., RAMAKRISHNAPPA, T., WANG, Y., WANG, L., SUN, T. and HU, X. 2018. Adsorption removal of methylene blue from aqueous solution on carbon-coated Fe3O4 microspheres functionalized with chloroacetic acid. Science and engineering of composite materials, 25(2), pages 353-361. Held on OpenAIR [online]. Available from: https://openair.rgu.ac.uk.

Zefei Zhang, Cholhwan Kim, Carlos Fernandez, Manickam Minakshi Sundaram, Thippeswamy Ramakrishnappa, Yuhong Wang, Linshan Wang*, Ting Sun and Xiaomin Hu

Adsorption removal of methylene blue from aqueous solution on carbon-coated Fe_3O_4 microspheres functionalized with chloroacetic acid

DOI 10.1515/secm-2016-0138
Received May 2, 2016; accepted July 23, 2016

Abstract: We report the preparation and employability of carbon-coated Fe_3O_4 (Fe_3O_4/C) microspheres functionalized with chloroacetic acid (CAA) for the removal of methylene blue (MB) in aqueous solution. The prepared magnetic microspheres (Fe_3O_4/C-CAA) were characterized by the following techniques: X-ray diffraction, transmission electron microscopy, Fourier-transform infrared spectrometer, vibrating sample magnetometry, and Brunauer-Emmett-Teller. The characterization results showed that Fe_3O_4/C microspheres were modified by CAA without any phase change. Fe_3O_4/C-CAA microspheres have higher adsorption capacity for MB compared to Fe_3O_4/C microspheres. The Langmuir, Freundlich, and Temkin adsorption models were applied to describe the equilibrium isotherms, and the Langmuir adsorption model fitted well with the equilibrium data. The pseudo-first-order and pseudo-second-order kinetic models were used to describe the kinetics data. However, the pseudo-second-order kinetic model fitted better with the adsorption kinetics data.

***Corresponding author: Linshan Wang,** College of Sciences, Northeastern University, Shenyang 110004, China, Phone: +86 13604045464, Fax: 86-24-83684533, e-mail: lswang@mail.neu.edu.cn
Zefei Zhang, Cholhwan Kim, Yuhong Wang and Ting Sun: College of Sciences, Northeastern University, Shenyang 110004, China
Carlos Fernandez: School of Pharmacy and Life Sciences, Robert Gordon University, Garthdee Road, Sir Ian Wood Building, Aberdeen AB107GJ, UK
Manickam Minakshi Sundaram: School of Engineering and Information Technology, Murdoch University, Murdoch, WA 6150, Australia
Thippeswamy Ramakrishnappa: Center for Nano and Material Science, Global Campus, Jain University, Jakkasandra (P), Kankapura (T), 560001 Bangalore, Karnataka, India
Xiaomin Hu: College of Resources and Civil Engineering, Northeastern University, Shenyang 110004, China

Keywords: adsorption; carbon-coated Fe_3O_4 nanoparticles; chloroacetic acid; methylene blue.

1 Introduction

Dyes are widely used in various industries such as textiles, pulp mills, paper, printing, leather, plastics, etc., causing water pollution [1]. Because most of the industrial dyes are very harmful to human health and the environment, numerous techniques were adopted for their removal from contaminated waters [2]. Among different dye removal techniques, adsorption has been considered as one of the most promising techniques for removing dyes from industrial wastewaters, due to its high efficiency, simplicity, and reusability [3, 4]. Recently, magnetic materials have attracted considerable attention as adsorbents because of their simple and fast separation properties under external magnetic fields [5–7]. Magnetite (Fe_3O_4) has been the most widely studied among all magnetic materials due to its easy preparation, easy surface modification, easy operation, good recoverability, and excellent dispersibility in aqueous solution [8]. Its functionality has been recognized as one of the most intriguing methods to control adsorption of the target molecules. Synthesis and application of functionalized magnetic particles have been a hot topic. Carbon is a versatile material for functionalization of magnetite, due to their chemical stability, biocompatibility, possibility of surface modification, and pore creation [9]. Many research groups have explored the magnetic materials functionalized by carbon-based materials such as C_{18} [10], graphene [11], graphene oxide [12], carbon nanotubes [13], and activated carbon [14]. As one of the carbon-functionalized magnetic materials, hydrophilic carbon-coated magnetic materials (Fe_3O_4/C) have gained great interest as a low-cost adsorbent. It has been prepared by the introduction of a carbon precursor such as

glucose onto the magnetic surface followed by carbonization with a hydrothermal reaction. Finally, it has been successfully used as an adsorbent for polycyclic aromatic hydrocarbons, pesticides, dyes, etc. [15–23]. However, many previous research works only focused on the synthesis and application of Fe_3O_4/C, and little work has been reported on their surface chemical modification for improvement of adsorption performance. In this study, a novel magnetic adsorbent was developed for the adsorption enhancement of dyes by the surface modification of Fe_3O_4/C, which is depicted in Figure 1. The modified Fe_3O_4/C (denoted as Fe_3O_4/C-CAA) was characterized by transmission electron microscopy (TEM), Fourier-transform infrared (FT-IR) spectrometry, X-ray diffraction (XRD), vibrating sample magnetometry (VSM), and Brunauer-Emmett-Teller (BET). Methylene blue (MB) was selected as the model dye, and its adsorption behaviors on Fe_3O_4/C-CAA were systematically evaluated.

2 Experimental

2.1 Materials

MB was purchased from Guangdong Xilong Chemical Company. All other chemicals were purchased from Sinopharm Chemical Reagent Co., Ltd. (Shenyang, China). All chemicals were of analytical grade and used as received without further purification. Only deionized water was used to prepare aqueous solutions in the experiments.

2.2 Preparation of Fe_3O_4 and Fe_3O_4/C microspheres

The preparation of Fe_3O_4 and Fe_3O_4/C microspheres was based on previously reported methods [21, 24]. $FeCl_3 \cdot 6H_2O$ (1.35 g) was added in ethylene glycol (40 ml) and stirred until $FeCl_3$ was dissolved completely, and then sodium acetate anhydrous (3.6 g) was added in the above mixture and stirred vigorously for 2 h. Then, the mixture was transferred into a Teflon-lined stainless-steel autoclave and kept at 200°C for 6 h. The obtained products were cooled naturally, washed with water and ethanol, and dried at 60°C. Fe_3O_4 microspheres (0.2 g) were ultrasonicated for 10 min in 0.1 M HNO_3 followed by washing with deionized water for several times and introduced in 30 ml glucose aqueous solution (0.5 M), and dispersed under vigorous stirring. After stirring for 30 min, the suspension was placed in a Teflon-sealed autoclave and kept at 180°C for 6 h, and cooled to room temperature. The obtained products were separated by a magnet, washed with water and ethanol several times, and dried at 60°C.

2.3 Modification of Fe_3O_4/C microspheres

The Fe_3O_4/C microspheres (0.2 g) were added into an aqueous solution of 0.01 M chloroacetic acid (30 ml). After stirring for 30 min, the mixture was heated to reflux for 1 h. Then, the suspension was cooled to room temperature and the obtained products (Fe_3O_4/C-CAA microspheres) were separated magnetically, washed with water several times, and then dried at 60°C.

2.4 Characterization of magnetic microspheres

The TEM images were determined on a Tecnai G220 microscope (Fei, USA) with an accelerating voltage of 200 kV. The crystal structure was characterized by an X'pert Pro diffractometer (PANalytical, Holland) with Cu Kα radiation (λ = 0.15406 nm) from 20° to 70°. FT-IR spectra in KBr were obtained by using Vertex70 FT-IR spectrometer (Bruker, Germany). The magnetic properties of Fe_3O_4/C and Fe_3O_4/C-CAA microspheres were measured using a vibration sample magnetometer with an applied field between –10 and +10 kOe at room temperature (Lakeshore, serial no.1740H, REV-127, USA). Nitrogen adsorption isotherms of the synthesized products were obtained from an ASAP 2020 HD 88 instrument.

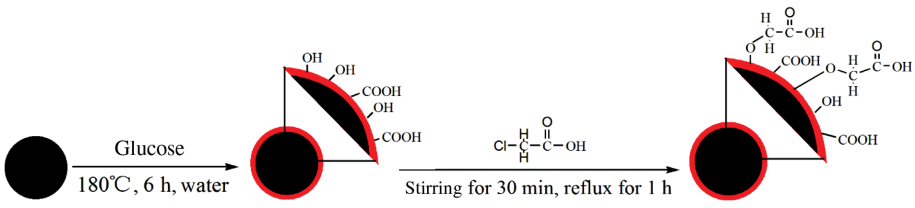

Figure 1: The modification of Fe_3O_4/C by CAA.

2.5 Adsorption of MB by Fe_3O_4/C-CAA microspheres and regeneration of adsorbents

Batch adsorption experiments were carried out to evaluate the adsorption ability of Fe_3O_4/C-CAA microspheres for MB removal from an aqueous solution. MB solutions of desired concentration were prepared by suitable dilution of the stock solution, and their pH was adjusted using a 0.1 M HCl or NaOH solution. The ionic strength of the solution was varied between 0 and 0.2 M using NaCl. Ten milligrams of the adsorbent was dispersed in 20 ml MB aqueous solution, and the suspension was shaken with an oscillator (150 rpm) for a certain time to reach equilibrium at 25°C. At preselected time intervals, Fe_3O_4/C-CAA microspheres were isolated from the solution using a magnet. The concentration of MB in solution was analyzed by using a TU-1900 UV-visible adsorption spectrophotometer (Beijing Purkinjie General Instrument Co., Ltd., Beijing, China) at 660 nm. The amount of MB adsorbed (q_t, mg g^{-1}) was calculated using the following equation:

$$\frac{1}{q_t} = \frac{K_1}{q_m t} + \frac{1}{q_m}, \quad (1)$$

where C_0 (mg l^{-1}) is the initial MB concentration, C_t (mg l^{-1}) is the MB concentration in the supernatant at time t (min), V (l) is the volume of MB solution used, and W (g) is the weight of Fe_3O_4/C-CAA microspheres used. The regeneration, recycle, and reuse of Fe_3O_4/C-CAA microspheres were investigated using ethanol as desorption media. The Fe_3O_4/C-CAA microspheres adsorbed with MB were magnetically separated and stirred in ethanol solution for another 120 min. The MB concentration in the desorption solution was analyzed spectrophotometrically. The Fe_3O_4/C-CAA microspheres were washed with water five times, dried, and reused for the removal of MB from aqueous solution.

3 Results and discussion

3.1 Characterization of Fe_3O_4/C-CAA microspheres

The TEM images of the synthesized Fe_3O_4/C and Fe_3O_4/C-CAA microspheres are shown in Figure 2A and B. Fe_3O_4/C and Fe_3O_4/C-CAA microspheres have a quasi-spherical shape and have nearly uniform distribution of particle size. Gray shells surrounding the dark core of Fe_3O_4 are observed in both magnetic microspheres, indicating a typical core/shell structure of Fe_3O_4/C and Fe_3O_4/C-CCA microspheres. The average diameter of Fe_3O_4/C-CAA microspheres is about 320 nm with the thickness of the shell of about 10 nm, which has no notable difference compared with that of Fe_3O_4/C microspheres. Energy dispersive spectrometry (EDS) maps show that the main components on the surface of Fe_3O_4/C (Figure 2C) and Fe_3O_4/C-CAA (Figure 2D) were identical, consisting of C, O, and Fe.

The XRD patterns of the prepared magnetic microspheres are shown in Figure 3. There is no apparent difference between the XRD patterns of Fe_3O_4/C and Fe_3O_4/C-CAA microspheres, and all observed diffraction peaks in the patterns of both magnetic microspheres are matched well in position and intensity with a cubic phase of Fe_3O_4 [25]. The result implies that the outer shell is amorphous

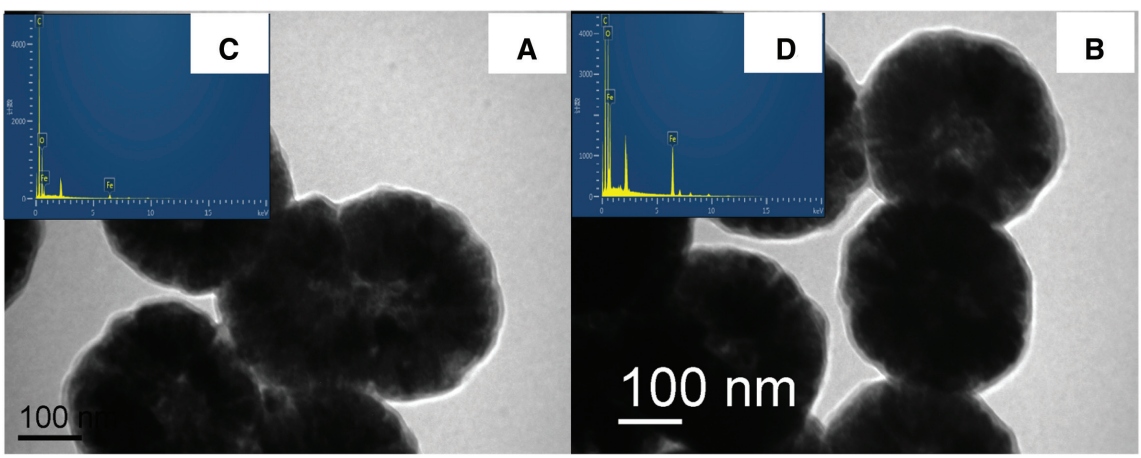

Figure 2: TEM and EDS images of Fe_3O_4/C (A) and Fe_3O_4/C-CAA (B) microspheres.

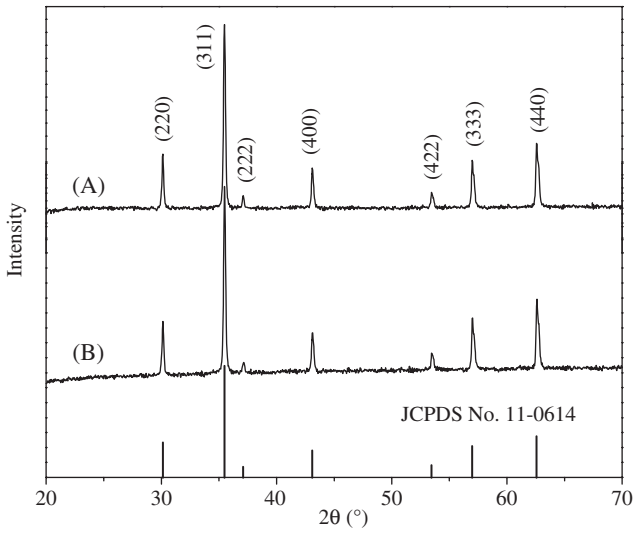

Figure 3: X-ray powder diffraction patterns for Fe_3O_4/C (A) and Fe_3O_4/C-CAA microspheres (B).

and carbon coating or modification by CAA does not change the crystal structure of magnetite.

Figure 4 shows the FT-IR spectra of Fe_3O_4/C and Fe_3O_4/C-CAA microspheres. The peaks at around 579 cm^{-1} are assigned to the stretching vibrations of Fe-O in the spectra of Fe_3O_4/C and Fe_3O_4/C-CAA microspheres. The peaks at around 1699, 1633, and 3429 cm^{-1} are assigned to stretching vibrations of C=O, C=C, and O-H, which are observed in both magnetic microspheres, respectively. After modification, a series of peaks at around 1116, 1274, and 1380 cm^{-1} appeared and the relative strength of the peak at 1699 cm^{-1} increased, which was due to the stretching vibration of C-OH groups, bending vibration of O-H, symmetrical stretching vibration of carboxylate group, and stretching vibration of C=O [21, 26, 27]. These results indicate that Fe_3O_4/C microspheres were successfully prepared and clearly modified by CAA. The surface of Fe_3O_4/C-CAA microspheres has more -COOH groups than that of Fe_3O_4/C microspheres, which could provide much more adsorption active sites for MB.

Figure 5 shows the VSM curves of Fe_3O_4/C and Fe_3O_4/C-CAA microspheres at room temperature. The maximal saturation magnetizations of Fe_3O_4/C and Fe_3O_4/C-CAA microspheres were 65.5 and 64.3 emu g^{-1}, respectively. The slight difference in maximal saturation magnetizations between the two kinds of magnetic microspheres can be attributed to the contribution of CAA bound on the surface of Fe_3O_4/C-CAA microspheres. There was no hysteresis in the hysteresis loop, and remanence and coercivity were zero. This illustrated that both magnetic microspheres were superparamagnetic.

The BET surface areas and the porosity of Fe_3O_4/C and Fe_3O_4/C-CAA microspheres were calculated from nitrogen adsorption isotherms (Figure 6A and B). The surface areas of Fe_3O_4/C and Fe_3O_4/C-CAA microspheres are 4.6354 and 4.9545 m^2 g^{-1}, respectively, and their pore volumes are 0.0125 and 0.0119 cm^3 g^{-1}, respectively.

In addition, their pore size distributions were all centered at about 26 nm. These results indicate that the modification of Fe_3O_4/C microspheres by CAA did not change their surface area and porosity greatly. The slight enhancement in specific surface area of Fe_3O_4/C-CAA microspheres may be ascribed to the increase of adsorption active sites caused by CAA modification.

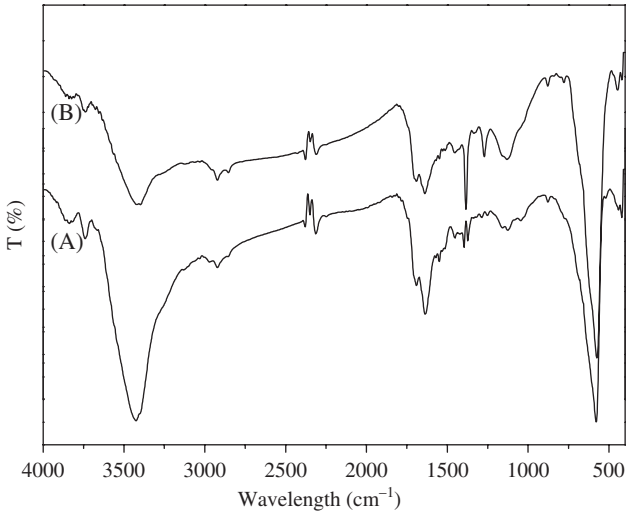

Figure 4: FT-IR spectra of Fe_3O_4/C (A) and Fe_3O_4/C-CAA microspheres (B).

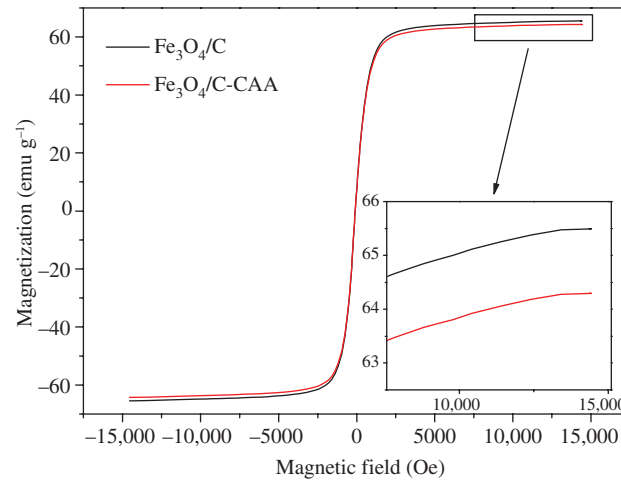

Figure 5: Magnetization curves of Fe_3O_4/C (A) and Fe_3O_4/C-CAA microspheres (B).

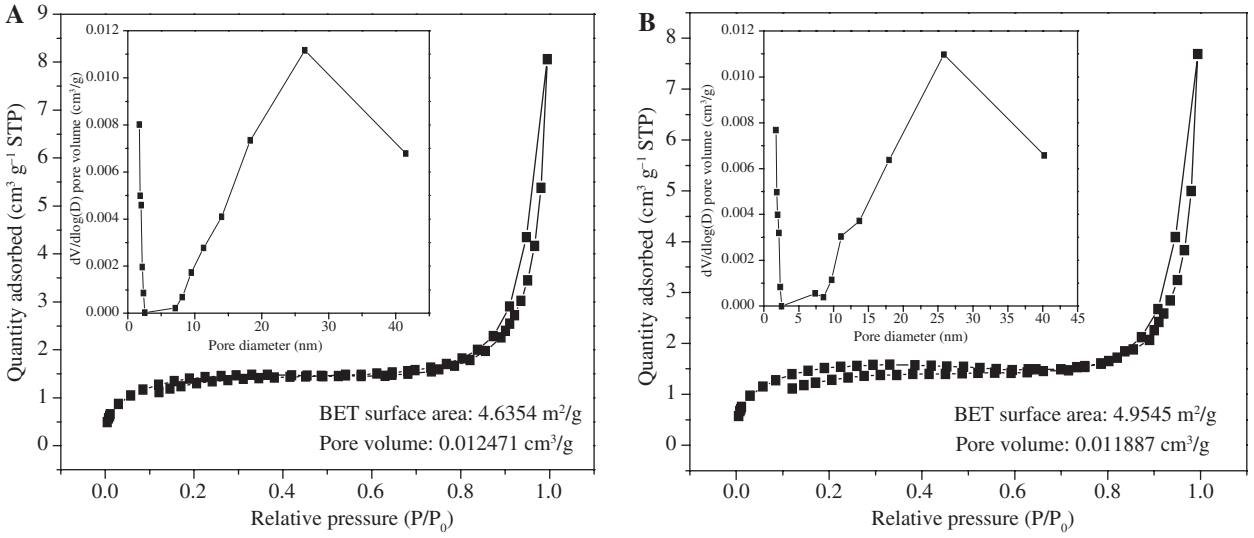

Figure 6: Nitrogen adsorption/desorption isotherms and pore size distribution (inset) of Fe_3O_4/C (A) and Fe_3O_4/C-CAA microspheres (B).

3.2 Adsorption properties of the Fe_3O_4/C-CAA microspheres

3.2.1 Effect of CAA concentration

The effect of CAA concentration on the adsorption of MB by Fe_3O_4/C-CAA microspheres was studied in 200 mg l^{-1} MB solution at pH 11 (Figure 7). As shown in Figure 7, the adsorption capacity of Fe_3O_4/C-CCA microspheres for MB increased with the increasing CAA concentration in aqueous solution, and the maximum adsorption amount was reached when Fe_3O_4/C was modified with 0.01 M CAA solution. With further increase of CAA concentration, the adsorption capacity slightly decreased, indicating that the moderate CAA concentration was beneficial to enhance the adsorption removal of MB onto Fe_3O_4/C-CAA microspheres. Thus, 0.01 M was selected as the optimum concentration.

3.2.2 Effect of pH

The effect of pH on the adsorption of MB by the Fe_3O_4/C and Fe_3O_4/C-CAA microspheres was investigated from pH 3 to 11 in 200 mg l^{-1} MB solution (Figure 8). The adsorption amount of MB onto the both magnetic microspheres

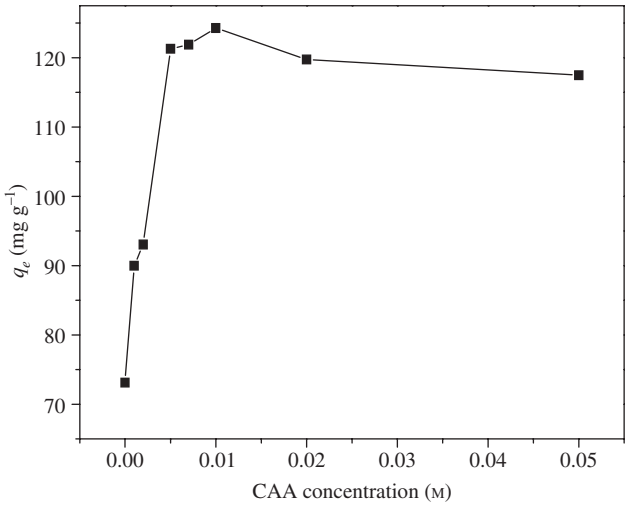

Figure 7: Effect of CAA concentration (when Fe_3O_4/C is modified with CAA) on the adsorption of MB by Fe_3O_4/C-CAA microspheres at pH 11 and 25°C.

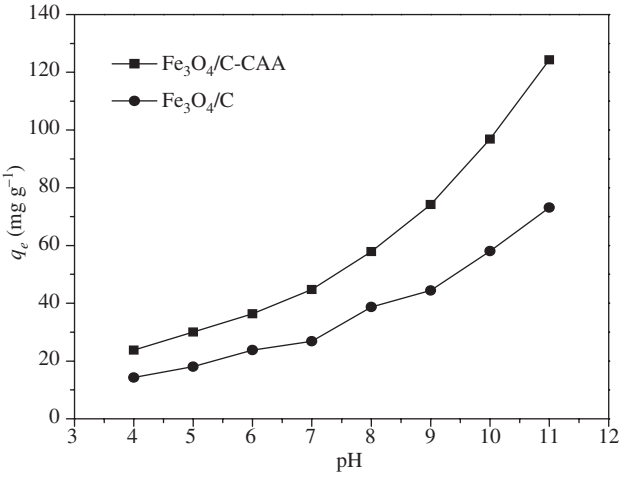

Figure 8: Effect of pH on the adsorption of MB by Fe_3O_4/C-CAA microspheres at 25°C.

increased with increasing pH of the solution over the range from 3.0 to 11.0. The higher adsorption amount at higher pH of solution was due to the deprotonation of the surface groups on magnetic microspheres. Thus, the stronger electrostatic interaction that existed between magnetic microspheres and MB enhanced the adsorption amount of MB on Fe_3O_4/C-CAA microspheres. The adsorption capacity of the Fe_3O_4/C-CAA microspheres was higher than that of Fe_3O_4/C over the whole range of pH 3–11, which could be due to the contribution of oxygen-containing groups added by CAA.

3.2.3 Effect of ionic strength on the adsorption

The effect of ionic strength on the adsorption of MB was investigated by adding NaCl in 200 mg l^{-1} of MB solution at pH 11 (Figure 9). Figure 9 illustrates the adsorption capacities of Fe_3O_4/C-CAA microspheres with MB, which significantly decreased with the increasing of NaCl concentration. This phenomenon is attributed to the competitive effect of Na^+ on binding sites, which increased with the NaCl concentration [28].

3.2.4 Adsorption kinetics

The effect of contact time on the adsorption of MB by Fe_3O_4/C-CAA microspheres was examined in 200 mg l^{-1} MB solution (pH 11). Figure 10 illustrates the effect of contact time on MB adsorption. It shows that the amount of adsorbed MB by Fe_3O_4/C-CAA microspheres increased

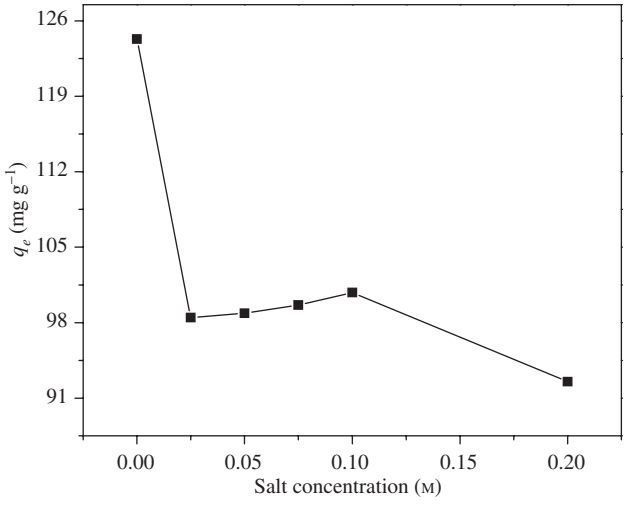

Figure 9: Effect of ionic strength on the adsorption of MB by Fe_3O_4/C-CAA microspheres at pH 11 and 25°C.

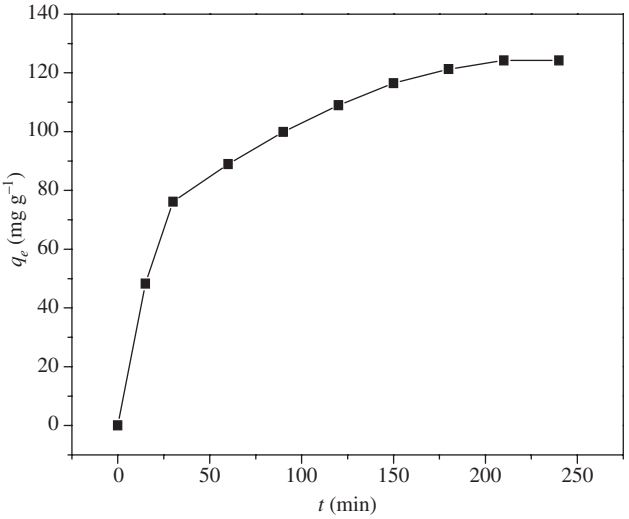

Figure 10: Effect of contact time on the adsorption of MB by Fe_3O_4/C-CAA microspheres at pH 11 and 25°C.

with increasing contact time. The adsorption achieved equilibrium within 210 min.

The adsorption time data were treated by pseudo-first-order and pseudo-second-order models. The pseudo-first-order model and pseudo-second-order model equations are expressed as follows [29, 30, 32]:

$$\text{Pseudo-first-order model: } \ln(q_m - q_t) = \ln q_m - K_1 t, \quad (2)$$

$$\text{Pseudo-second-order model: } \frac{t}{q_t} = \frac{1}{K_2 q_m^2} + \frac{t}{q_m}, \quad (3)$$

where q_m is the maximum adsorption capacity per unit weight of adsorbent (mg g^{-1}), q_t is the amount (mg g^{-1}) of MB adsorbed at time t (min), K_1 is the pseudo-first-order rate constant of adsorption (min^{-1}), and K_2 is the pseudo-second-order rate constant of adsorption (g mg^{-1} min^{-1}).

The kinetic constants using the pseudo-first-order and pseudo-second-order kinetic models are shown in Table 1.

As shown in Table 1, the calculated correlation coefficient ($R^2 = 0.9977$) of the pseudo-second-order model was higher than that of the pseudo-first-order model ($R^2 = 0.9738$). These results indicate that the pseudo-second-order model fitted well with the experimental data and could be used to describe the adsorption kinetics of MB onto Fe_3O_4/C-CAA microspheres (Figure 11).

3.2.5 Adsorption isotherms

The adsorption of MB by Fe_3O_4/C and Fe_3O_4/C-CAA microspheres were studied in MB solution (pH 11) with various

Table 1: Pseudo-first-order and pseudo-second-order kinetic constants for MB adsorption.

$q_{e,exp}$ (mg g^{-1})	Pseudo-first			Pseudo-second		
	$q_{m,cal}$ (mg g^{-1})	K_1 (min^{-1})	R^2	$q_{m,cal}$ (mg g^{-1})	K_2 (g mg^{-1} min^{-1})	R^2
124.28	108.86	1.84×10^{-2}	0.9738	140.67	2.29×10^{-4}	0.9977

$q_{e,exp}$ is equilibrium adsorption capacity. $q_{m,cal}$ is maximum adsorption capacity calculated according to kinetic models.

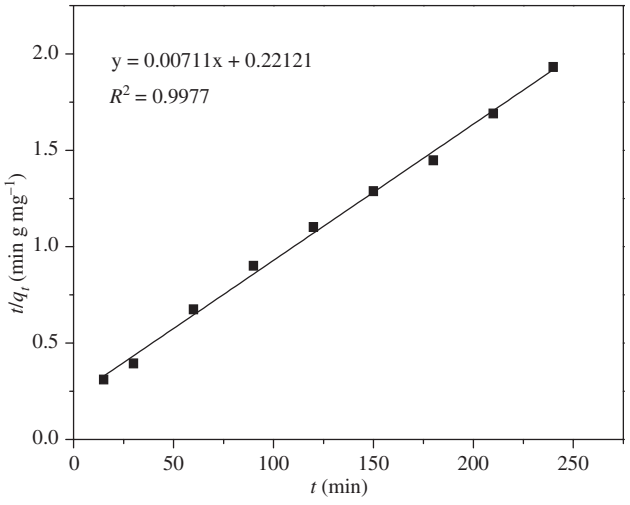

Figure 11: The plot of pseudo-second-order model of Fe_3O_4/C-CAA microspheres.

concentrations ranging from 0 to 250 mg l^{-1} for 210 min at 25°C (Figure 12). As shown in Figure 12, the adsorbed amounts of MB on Fe_3O_4/C-CAA microspheres increased rapidly from 0 to <200 mg l^{-1} with the MB concentrations.

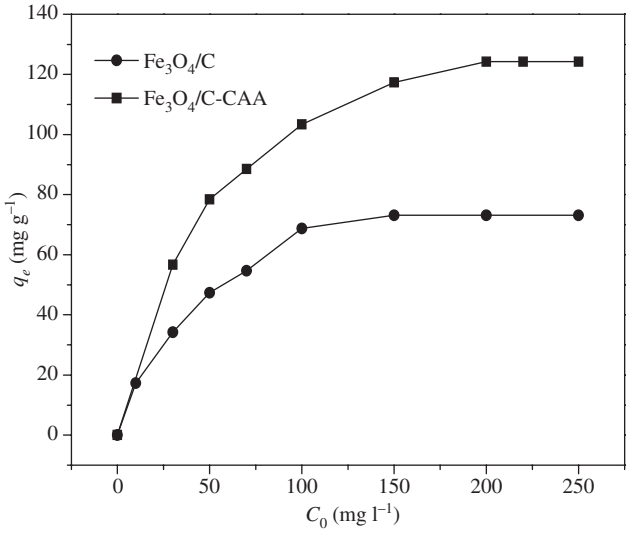

Figure 12: The effect of initial MB concentration on the adsorption of MB by Fe_3O_4/C and Fe_3O_4/C-CAA microspheres at pH 11 and 25°C.

At concentrations >200 mg l^{-1}, the amount tended to stabilize. When the initial concentration of MB was >200 mg l^{-1}, the maximum adsorption was achieved and the adsorbed amount of MB on Fe_3O_4/C-CAA microspheres was 124.28 mg g^{-1}, which is 1.7 times higher than that on the Fe_3O_4/C microspheres (73.1 mg g^{-1}).

The experimental data for adsorbed MB on Fe_3O_4/C-CAA microspheres were analyzed using the Langmuir, Freundlich, and Temkin models [30–32].

The equations are listed below:

$$\text{Langmuir model: } \frac{C_e}{q_e}=\frac{C_e}{q_m}+\frac{1}{q_mK_L}, \tag{4}$$

$$\text{Freundlich model: } \ln q_e=\ln K_F+\frac{1}{n}\ln C_e, \tag{5}$$

$$\text{Temkin model: } q_e=B\ln K_T+B\ln C_e, \tag{6}$$

where q_e is the equilibrium adsorption capacity per unit weight of adsorbent (mg g^{-1}); C_e is the equilibrium concentration (mg l^{-1}); K_L is the Langmuir equilibrium adsorption constant (l mg^{-1}); q_m is the theoretical maximum adsorption capacity per unit weight of adsorbent (mg g^{-1}); K_F, n are the Freundlich constants; and K_T, B are Temkin constants. The calculated constants in the three isotherm models are presented in Table 2.

The adsorption data of MB adsorbed on Fe_3O_4/C-CAA microspheres were found to fit better to the Langmuir model with an R^2 value of 0.9981, higher than those of the Freundlich model (R^2 = 0.9515) and the Temkin model (R^2 = 0.9819), indicating that the Langmuir model better describes the adsorption behavior of MB on Fe_3O_4/C-CAA microspheres (Figure 13).

The maximum adsorption capacity (q_m) of Fe_3O_4/C-CAA from the Langmuir model was calculated to be about 150.60 mg g^{-1}, which was higher than those of other materials published in the literature [21, 23, 33, 34] (Table 3). Due to their good adsorption performance on dyes and easy separation under an external magnetic field, superparamagnetic Fe_3O_4/C composite materials have been considered as promising adsorbents for removing organic dyes from polluted water [21, 23]. CAA-modified Fe_3O_4/C,

Table 2: Adsorption isotherm constants for MB adsorption.

$q_{e,exp}$ (mg g^{-1})	Langmuir constants			Freundlich constants			Temkin constants		
	q_m (mg g^{-1})	K_L (l mg^{-1})	R^2	K_F	n	R^2	B	K_T	R^2
124.28	150.60	2.13×10^{-2}	0.9981	18.33	2.77	0.9515	32.79	0.21	0.9819

$q_{e,exp}$ is equilibrium adsorption capacity. q_m is maximum adsorption capacity calculated according to the isotherm model.

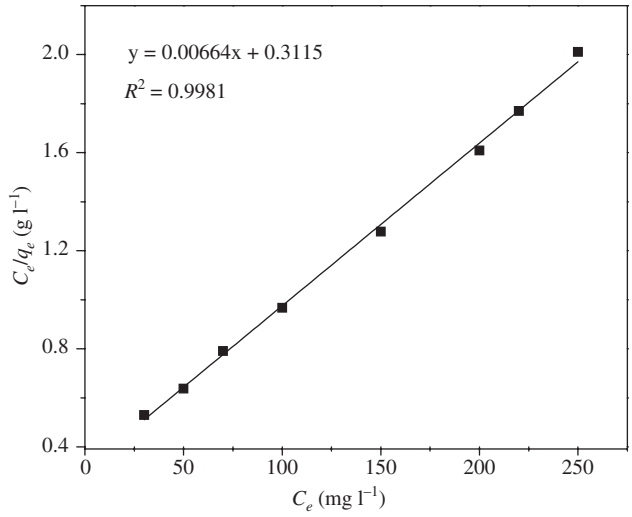

Figure 13: The plot of the Langmuir isotherm model of Fe_3O_4/C-CAA microspheres.

Table 3: Comparison of adsorption ability with different adsorbents.

Adsorbents	Adsorption capacity for MB	Reference
Fe_3O_4@C obtained by a two-step method	44.38 mg g^{-1}	[21]
Fe_3O_4@C obtained by direct precipitation method	117 mg g^{-1}	[23]
Fe_3O_4-MWCNT composites	40.06 mg g^{-1}	[33]
Porous magnetic manganese oxide nanostructures	70 mg g^{-1}	[34]
Fe_3O_4/C-CAA	150.60 mg g^{-1}	This study

denoted as Fe_3O_4/C-CAA in this study, demonstrated better adsorption capacity for MB than Fe_3O_4/C. It is reasonable to suggest that Fe_3O_4/C-CAA microspheres are promising adsorbents applicable for removing dyes from waters.

3.2.6 Regeneration and reuse of Fe_3O_4/C-CAA microspheres

In order to test the regeneration and reusability of Fe_3O_4/C-CAA microspheres, the MB adsorption-desorption cycle was repeated four times using the same magnetic microspheres (Figure 14). As shown in Figure 14, at the fourth cycle, the relative adsorption capacity of Fe_3O_4/C-CAA for MB was 88.5%, much higher than that of Fe_3O_4/C whose relative adsorption capacity for MB decreased to 59.0% at the fourth cycle [23]. Fe_3O_4/C-CAA showed good reusability for MB adsorption.

4 Conclusions

Fe_3O_4/C microspheres functionalized with CAA were successfully prepared, and their adsorption ability was evaluated for MB. Fe_3O_4/C-CAA microspheres have higher adsorption capacity than Fe_3O_4/C microspheres for MB. The adsorption equilibrium was reached within 210 min, and the adsorption kinetics of MB on Fe_3O_4/C-CAA microspheres was described by the pseudo-second-order model. The Langmuir isotherm model better describes the adsorption behavior of MB than does the Freundlich isotherm model or the Temkin isotherm model, and the maximum adsorption capacity calculated from Langmuir

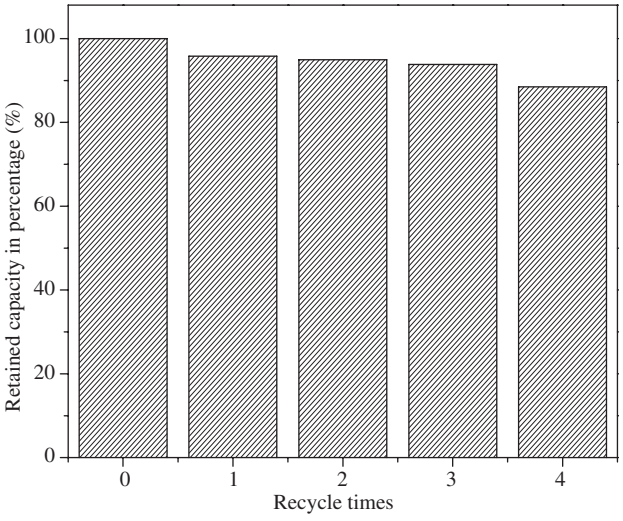

Figure 14: The adsorption amounts of MB over Fe_3O_4/C-CAA microspheres for different recycle numbers.

isotherm model was about 150.60 mg g^{-1}. Fe_3O_4/C-CAA microspheres have good recycling ability for MB.

Acknowledgments: The authors are grateful for the financial aid from the Major Science and Technology Program for Water Pollution Control and Treatment (no. 2013ZX07202-010).

References

[1] Qu LL, Han TT, Luo ZJ, Liu CC, Mei Y, Zhu T. *J. Phys. Chem. Solids* 2015, 78, 20–27.
[2] Gupta VK, Suhas. *J. Environ. Manage.* 2009, 90, 2313–2342.
[3] Tajizadegan H, Jafari M, Rashidzadeh M, Saffar-Teluri A. *Appl. Surf. Sci.* 2013, 276, 317–322.
[4] Boruah PK, Borah DJ, Handique J, Sharma P, Sengupta P, Das MR. *J. Environ. Chem. Eng.* 2015, 3, 1974–1985.
[5] Mehta D, Mazumdar S, Singh SK. *J. Water Process Eng.* 2015, 7, 244–265.
[6] Ozmen M, Can K, Arslan G, Tor A, Cengeloglu Y, Ersoz M. *Desalination* 2010, 254, 162–169.
[7] Can K, Ozmen M, Ersoz M. *Colloid Surf. B* 2009, 71, 154–159.
[8] Li XS, Zhu GT, Luo YB, Yuan BF, Feng YQ. *Trends Anal. Chem.* 2013, 45, 234–247.
[9] Tristão JC, Oliveira AAS, Ardisson JD, Dias A, Lago RM. *Mater. Res. Bull.* 2011, 46, 748–754.
[10] Hsiao HH, Hsieh HY, Chou CC, Lin SY, Wang AHJ, Khoo KH. *J. Proteome Res.* 2007, 6, 1313–1324.
[11] Yao YJ, Miao SD, Liu SZ, Ma LP, Sun HQ, Wang SB. *Chem. Eng. J.* 2012, 184, 326–332.
[12] Deng JH, Zhang XR, Zeng GM, Gong JL, Niu QY, Liang J. *Chem. Eng. J.* 2013, 226, 189–200.
[13] Sun XS, Ou HJ, Miao CF, Chen LG. *Mater. Res. Bull.* 2015, 70, 82–86.
[14] Do MH, Phan NH, Nguyen TD, Pham TTS, Nguyen VK, Vu TTT, Nguyen TKP. *Chemosphere* 2011, 85, 1269–1276.
[15] Zhang SX, Niu HY, Hu ZJ, Cai YQ, Shi YL. *J. Chromatogr. A* 2010, 1217, 4757–4764.
[16] Yang J, Li JY, Qiao JQ, Lian HZ, Chen HY. *J. Chromatogr. A* 2014, 1325, 8–15.
[17] Yang J, Li JY, Qiao JQ, Cui SH, Lian HZ, Chen HY. *Appl. Surf. Sci.* 2014, 321, 126–135.
[18] Shen R, Yang F, Wang J, Li Y, Xie S, Chen C, Cai Q, Yao S. *Anal. Methods* 2011, 3, 2909–2914.
[19] Heidari H, Razmi H. *Talanta* 2012, 99, 13–21.
[20] Bao XL, Qiang ZM, Chang JH, Ben WW, Qu JH. *J. Environ. Sci.* 2014, 26, 962–969.
[21] Zhang ZY, Kong JL. *J. Hazard. Mater.* 2011, 193, 325–329.
[22] Qu LL, Han TT, Luo ZJ, Liu CC, Mei Y, Zhu T. *J. Phys. Chem. Solids* 2015, 78, 20–27.
[23] Wu RH, Liu JH, Zhao LQ, Zhang XL, Xie JR, Yu BW, Ma XL, Yang ST, Wang HF, Liu YF. *J. Environ. Chem. Eng.* 2014, 2, 907–913.
[24] Deng H, Li X, Peng Q, Wang X, Chen J, Li Y. *Angew. Chem. Int. Ed.* 2005, 44, 2782–2785.
[25] Tang HJ, Han TT, Luo ZJ, Wu XY. *Chin. Chem. Lett.* 2013, 24, 63–66.
[26] Yang SX, Wang LY, Zhang XD, Yang WJ, Song GL. *Chem. Eng. J.* 2015, 275, 315–321.
[27] Chen QC, Wu QS. *J. Hazard. Mater.* 2015, 283, 193–201.
[28] Chen H, Zhao J, Dai GL. *J. Hazard. Mater.* 2011, 186, 1320–1327.
[29] Kannan N, Sundaram MM. *Dyes Pigments* 2001, 51, 25–40.
[30] Sun J, Su YJ, Rao SQ, Yang YJ. *J. Chromatogr. B* 2011, 879, 2194–2200.
[31] Lawal OS, Sanni AR, Ajayi IA, Rabiu OO. *J. Hazard. Mater.* 2010, 177, 829–835.
[32] Ozmen M, Can K, Akin I, Arslan G, Tor A, Cengeloglu Y, Ersoz M. *J. Hazard. Mater.* 2009, 171, 594–600.
[33] Ai LH, Zhang CY, Liao F, Wang Y, Li M, Meng LY, Jiang J. *J. Hazard. Mater.* 2011, 198, 282–290.
[34] Chen HM, Chu PK, He JH, Hu T, Yang MQ. *J. Colloid Interface Sci.* 2011, 359, 68–74.